Sedimentary Geology 231 (2010) 74–84

Contents lists available at ScienceDirect

Sedimentary Geology

journal homepage: www.elsevier.com/locate/sedgeo

Provenance of the Liuqu Conglomerate in southern Tibet: A Paleogene erosional record of the Himalayan–Tibetan orogen

Jian-Gang Wang [a], Xiu-Mian Hu [a,*], Fu-Yuan Wu [b], Luba Jansa [c,d]

[a] State Key Laboratory of Mineral Deposits Research, School of Earth Sciences and Engineering, Nanjing University, Nanjing 210093, China
[b] Institute of Geology and Geophysics, Chinese Academy of Sciences, Beijing 100029, China
[c] Geological Survey of Canada, Dartmouth, N.S., Canada
[d] Department of Earth Sciences, Dalhousie University, Halifax, N.S., Canada

ARTICLE INFO

Article history:
Received 7 January 2010
Received in revised form 20 July 2010
Accepted 3 September 2010
Available online 15 September 2010

Editor: G.J. Weltje

Keywords:
Liuqu Conglomerate
Himalayan–Tibetan orogen
Erosion
Southern Tibet
Hf isotope provenance
Detrital geochronology

ABSTRACT

The Liuqu Conglomerate, exposed along the Yarlung-Zangbo suture zone in southern Tibet, has been interpreted as a Paleogene molasse deposited during India–Asia collision or the product of collision between India and an intra-oceanic arc. Detailed petrographic studies and analyses of U–Pb and Hf isotopes of detrital zircon indicate multiple sources for the conglomerate, including the sedimentary succession within the Xigaze forearc basin to the north of the suture, the Yarlung-Zangbo ophiolite within the suture itself, and the Langjiexue Group and Tethyan Himalayan sedimentary rocks to the south of the suture. The occurrence of clasts of both Indian and Asian origin suggests that the conglomerate was deposited after India–Asia collision. The present data suggest that the onset of Himalayan–Tibetan orogenic erosion occurred as early as the Middle Eocene, when the Yarlung-Zangbo suture zone and Xigaze forearc succession were uplifted and became sources for the Liuqu Conglomerate. Thus, the results are inconsistent with the proposal that the provenance and age of the Liuqu Conglomerate support the hypothesis that India–Asia collision did not occur until the Oligocene. It is further suggested that Eocene Neotethyan slab breakoff, which may result in accelerated exhumation and uplift of the orogen, provided a deep-level dynamic control on the deposition of the Liuqu Conglomerate.

1. Introduction

An understanding of the history of Himalayan–Tibetan orogenic erosion is critical for deciphering crustal deformation processes and for investigating the proposed link between erosion of the orogen and changes in both global climate and ocean geochemistry (Najman et al., 2008). Investigation of the sedimentary record of material eroded from the mountain belt is a commonly used approach to determine the timing of India–Asia collision, constrained by the first arrival of Asian detritus on the Indian plate, or the earliest evidence of mixed Indian–Asian detritus (Najman, 2006). In the east-central Himalaya, Asian-derived detritus is first found on the Indian plate within Early Eocene marine strata (Wang et al., 2002; Ding et al., 2005; Zhu et al., 2005), while a significant input of Himalayan orogenic material into the foreland basin occurred during the Early Miocene (~21 Ma) (Burbank et al., 1996; Najman et al., 2004).

The occurrence of Paleogene molasse along the Yarlung-Zangbo suture zone in southern Tibet is poorly documented, although two distinct molasse belts have been reported (e.g., Yin et al., 1988; Harrison et al., 1993; Einsele et al., 1994; Wang et al., 1999, 2000; Li et al., 2010). The interior molasse belt, known by a variety of local stratigraphic names including the Kailas, Qiabulin, Dazhuqu, and Luobusa formations, is considered to record Late Oligocene–Miocene tectonic events (Harrison et al., 1993; Aitchison et al., 2002). The exterior molasse belt, named the Liuqu Conglomerate, is considered to represent a continental molasse deposited after India–Asia collision (Yin et al., 1988; Fang et al., 2006), which is commonly taken as having occurred at 55–50 Ma (e.g., Klootwijk et al., 1992; Searle et al., 1997; Zhu et al., 2005). However, Aitchison et al. (2000) cited the reported lack of Asian-derived detritus in the Liuqu Conglomerate to support their theory that India–Asia collision did not occur until the Oligocene, and that the conglomerate resulted from collision not between India and Asia, but between India and an intra-oceanic arc which occurred at this time (Aitchison et al., 2000, 2007a; Davis et al., 2002).

A lack of understanding of the record of Paleogene orogenic erosion in the east-central Himalaya has contributed to the controversy regarding the timing and nature of India–Asia collision and Himalayan–Tibetan orogenesis (e.g., Rowley, 1996; Najman and Garzanti, 2000; Najman et al., 2008). Thus, in the present study, we carried out a detailed provenance study on the Liuqu Conglomerate, with the aim of reliably constraining the sedimentary provenance of

* Corresponding author. Tel.: +86 25 83593002; fax: +86 25 83686016.
E-mail addresses: gang.0721@163.com (J.-G. Wang), huxm@nju.edu.cn (X.-M. Hu), wufuyuan@mail.igcas.ac.cn (F.-Y. Wu), lujansa@nrcan.gc.ca (L. Jansa).

0037-0738/$ – see front matter © 2010 Elsevier B.V. All rights reserved.
doi:10.1016/j.sedgeo.2010.09.004

the conglomerate and providing insight into the Paleogene erosional history of the Himalayan–Tibetan orogen and its tectonic significance. Although a previous, detailed lithological and sedimentological study of the Liuqu Conglomerate (Davis et al., 2002) has been conducted and used to support the hypothesis of collision between India and an intra-oceanic arc, this provenance study was based solely on petrographic observations and an analysis of clast lithology. To extend and test the findings of this earlier study, we undertook detailed petrographic studies and analyses of U–Pb and Hf isotopes of detrital zircon from sandstone and gravel within the Liuqu Conglomerate.

2. Geological setting

The Yarlung-Zangbo suture zone in southern Tibet, represented by E–W-trending ophiolite and serpentinite-matrix mélange, is considered to delineate the contact between the Indian and Asian continents (Fig. 1) (Hodges, 2000; Yin and Harrison, 2000; Dubois-Coté et al., 2005). North of the suture zone is the Lhasa Terrane, which consists primarily of Paleozoic and Mesozoic sedimentary strata associated with igneous rocks. The latter include volcanics and widespread intrusive bodies that have been divided into two suites: (1) a southern magmatic belt termed the Gangdese batholiths, which comprises Late Jurassic to Paleogene calc-alkaline granitic batholiths associated with the pre-collisional active southern margin of Asia (Chung et al., 2005; Chu et al., 2006; Wen et al., 2008; Ji et al., 2009), and (2) a northern magmatic belt that includes Early Cretaceous peraluminous (S-type) granitoids (Pan and Ding, 2004). The Paleogene Linzizong volcanic successions are widespread within the Lhasa terrane and unconformably overlie Paleozoic and Mesozoic sedimentary sequences and Gangdese batholiths (Lee et al., 2007, 2009; Mo et al., 2008). The Xigaze forearc basin, which lies at the southern margin of the Lhasa terrane, is considered to be the forearc to the southern active margin of the Asian plate and comprises Cretaceous clastic flysch interbedded with scarce marly carbonate layers (Einsele et al., 1994; Dürr, 1996; Wang et al., 1999) (Fig. 1).

South of the Yarlung-Zangbo suture zone, the Indian continent consists of the Tethyan, Higher, and Lesser Himalayas (Fig. 1a). The sedimentary sequence of the Tethyan Himalaya extends from the Paleozoic to the Eocene, comprising both clastic and carbonate rocks (Liu and Einsele, 1994; Willems et al., 1996; Jadoul et al., 1998; Garzanti, 1999). Within the sedimentary sequence, Early Paleozoic granites and Miocene leucogranites are exposed in a series of metamorphic core complexes (Hodges, 2000). South of the Tethyan Himalaya, separated by the south Tibetan detachment zone (STDZ), is the Higher Himalaya, comprising metamorphosed Proterozoic–Cambrian sedimentary rocks. The Main Central Thrust (MCT) separates the Higher Himalaya from the Lesser Himalaya to the south, which consists of un-metamorphosed and low-grade metamorphic crustal rocks of the Indian continent, mainly Precambrian to Paleozoic in age (Hodges, 2000; Yin, 2006). South of the Lesser Himalaya occurs the sub-Himalaya foreland basin, filled with Tertiary sedimentary rocks (Najman, 2006).

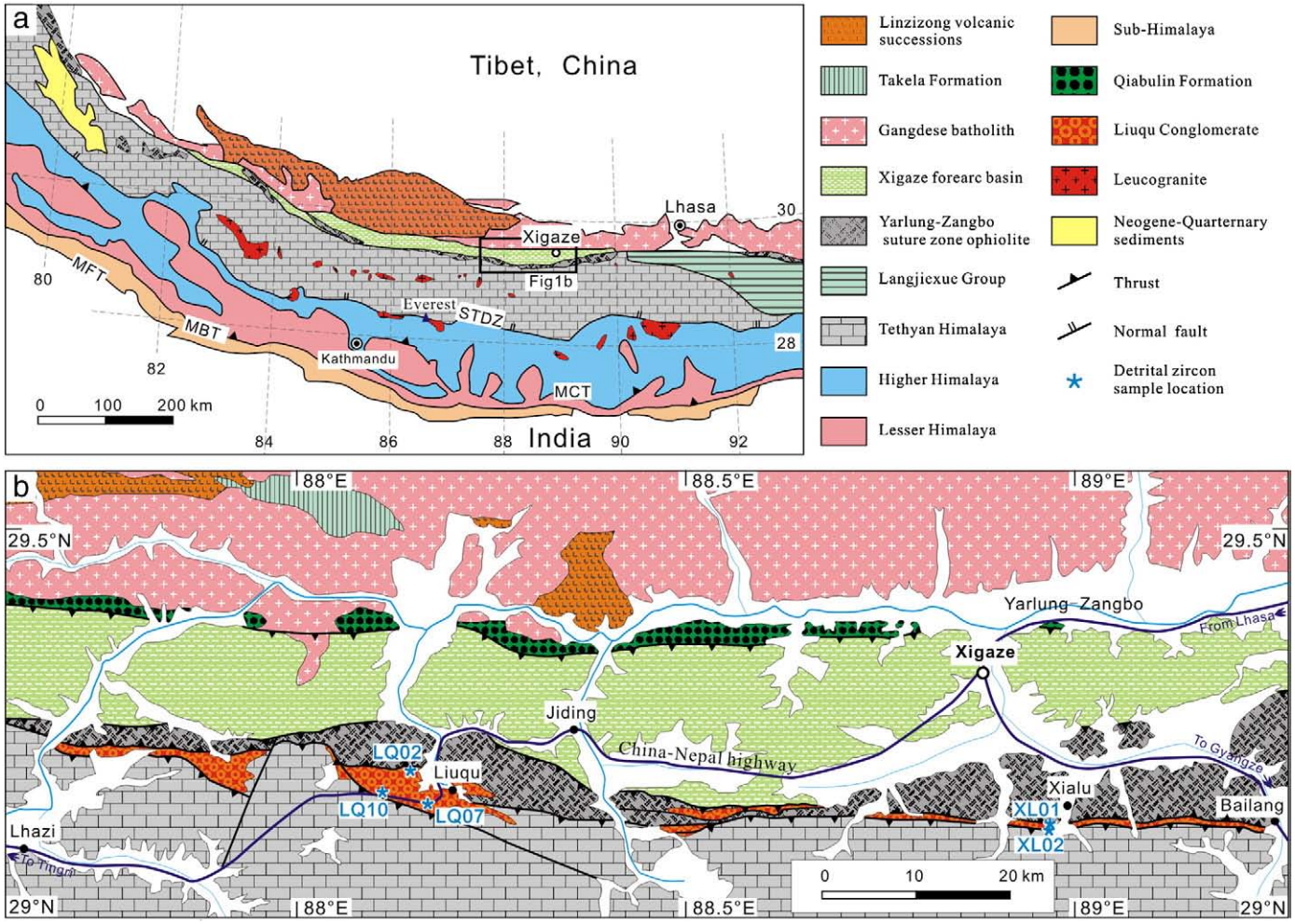

Fig. 1. a, Simplified tectonic map of the Himalaya and southern Tibet, modified after Yin and Harrison (2000). b, Geological sketch map of the Xigaze area, southern Tibet, modified after a 1:1,500,000 geologic map (Pan and Ding, 2004). Localities of samples for zircon dating are shown. STDZ, south Tibet detachment zone; MCT, main central thrust; MBT, main boundary thrust; MFT, main frontal thrust.

Within the eastern Himalaya, the Langjiexue Group, comprising Triassic sandstone and shale, has traditionally been assigned to the Tethyan Himalayan sedimentary province (Fig. 1a). However, recent studies have reported southward paleocurrent directions within the Langjiexue Group (Li et al., 2003). Whole-rock $\varepsilon_{Nd}(T)$ values (Dai et al., 2008) and detrital zircon ages obtained from these rocks (Aikman et al., 2008) differ from those of the Tethyan Himalaya (Gehrels et al., 2003; Hu et al., 2010) and the Xigaze forearc basin (Wu et al., 2010). This ambiguity has resulted in debate as to whether the Langjiexue Group should be assigned to the Tethyan Himalaya of the Indian plate (Liu and Einsele, 1994; Pan and Ding, 2004; Aikman et al., 2008), the sedimentary sequences of the Asian plate (Dai et al., 2008), or the Yarlung-Zangbo mélange (Yin, 2006; Aitchison et al., 2007a).

The Liuqu Conglomerate, which is the focus of the present study, extends over a distance of 150 km along the Yarlung-Zangbo suture zone near Xigaze (Fig. 1b). The conglomerate unconformably overlies, or is in a fault contact with, the Yarlung-Zangbo ophiolite to the north and the Triassic–Cretaceous low-grade metasedimentary rocks of the Tethyan sequences to the south (Yin et al., 1988). The total thickness of the Liuqu Conglomerate is up to 3500 m (Davis et al., 2002), although this varies among outcrops. The conglomerate is generally bedded at a scale of several centimeters up to 4 m, but is locally massive. Conglomerate beds are predominantly reddish in color, with some being light green. Davis et al. (2002) provided a detailed lithological description of the Liuqu Conglomerate at various localities along the Yarlung-Zangbo suture zone, and inferred deposition in a variety of settings from alluvial fan and braided river to subaqueous.

The age of the Liuqu Conglomerate is not well constrained because of a lack of age-diagnostic fossils. Several genera and species of plant fossils have been found at the Liuqu locality, including *Platanus* cf. *comstoki*, *Platanus* sp., *Corylites megaphylla*, *Corylites* sp., *Populusgigantophylla*, *Ficus* sp., *Mallotus* sp., *Grewiopsis* sp., *Grewia* sp., *Cissites* sp., *Cornophyllum* cf. *swidiformis*, *Phyllites* sp. A, *Phyllites* sp. B, and *Carpithes* sp., indicating an age of Middle to Late Eocene (Tao, 1988; Fang et al., 2006). A recent palynological study of the Liuqu Conglomerate yielded a Late Paleogene age (Wei et al., 2009). The sample analyzed in the present study yielded a single detrital zircon U–Pb age of 58 ± 1 Ma, which provides a maximum age constraint for the Liuqu Conglomerate. Taken together, the aforementioned age data indicate that the Liuqu Conglomerate was most probably deposited in the Middle–Late Eocene.

3. Samples and methods

This study focuses on the Liuqu Conglomerate exposed at the Liuqu and Xialu localities. The Liuqu section (LQ; 29°08′47″N, 88°09′06″E, elevation 4081 m) is located about 1 km west of Liuqu village in Lhatse County. Observations were mainly carried out along the China–Nepal Highway. The Xialu section (XL; 29°06′09″N, 88°58′7″E, elevation 4023 m) is exposed on the west side of the Xialu Valley in Bainang County. Twenty-two samples of sandstone and gravel were collected from different horizons, from which thin sections were prepared for petrographic analysis. Five samples, comprising four samples of sandstone (LQ07, LQ10, XL01, and XL02) and one sample of litharenitic gravel (LQ02), were selected for isotopic analyses of detrital zircons (Fig. 1b). All five samples were subjected to detrital U–Pb dating (Table A1), while zircons from samples LQ07 and XL01, and young zircons from samples LQ10 and XL02, were selected for analyses of Lu–Hf isotopes (Table A2).

Zircons were randomly hand-picked from heavy mineral concentrations and then encased in epoxy mounts and polished to expose their cores. Cathodoluminescence (CL) images were obtained to reveal internal structures and to select spots for analyses (Fig. A1). U–Pb dating of detrital zircon was performed by laser ablation–inductively coupled plasma–mass spectrometry (LA–ICP–MS) at the State Key Laboratory of Mineral Deposit Research, Nanjing University, China (for samples LQ02, LQ10, and XL02) and at the State Key Laboratory of Lithosphere Evolution, Institute of Geology of Geophysics, Chinese Academy of Sciences (for samples LQ07 and XL01), following the method described by Jackson et al. (2004). Various spot diameters (25, 30, 40, or 50 μm) were used depending on the grain size of zircon. In this study, interpretations of zircon ages are based on $^{206}Pb/^{238}U$ ages for grains younger than 1000 Ma and $^{207}Pb/^{206}Pb$ ages for grains older than 1000 Ma, as $^{206}Pb/^{238}U$ ages are generally more precise for younger ages, whereas $^{207}Pb/^{206}Pb$ ages are more precise for older ages.

Hf isotope analyses of detrital zircons were performed using a Neptune multiple collector–inductively coupled plasma–mass spectrometer (MC–ICP–MS) equipped with a 193 nm laser, housed at the State Key Laboratory of Lithosphere Evolution, Institute of Geology of Geophysics, Chinese Academy of Sciences. Details on instrumental conditions and data acquisition can be found in Wu et al. (2006). In this study, the $^{176}Hf/^{177}Hf$ ratio of standard zircon (91500) was 0.282278 ± 7 (2σ; MSWD = 0.81, n = 38), consistent with the value obtained previously in this laboratory (0.282307 ± 31) (Wu et al., 2006). To enable comparison among laboratories, all the Hf isotopic data were corrected by adjusting the $^{176}Hf/^{177}Hf$ ratio of 91500 to 0.282305. During the calculation, we adopted a depleted mantle model with $(^{176}Hf/^{177}Hf)_{DM} = 0.28325$ and $(^{176}Lu/^{177}Hf)_{DM} = 0.0384$ (Griffin et al., 2000); chondrite with $(^{176}Hf/^{177}Hf)_{CHUR} = 0.282772$ and $(^{176}Lu/^{177}Hf)_{CHUR} = 0.0332$ (BlichertToft and Albarede, 1997); and average continental crust with $(^{176}Lu/^{177}Hf)_C = 0.015$ (Griffin et al., 2002). We used a decay constant for ^{176}Lu of 1.867×10^{-11} (Soederlund et al., 2004).

4. Results

4.1. Petrography

Conglomerate is the major lithofacies in the Liuqu Conglomerate. Clasts are of polymictic composition, varying among outcrops, but are dominantly quartz-arenite, litharenite, basalt, radiolarian chert, phyllite, and slate, along with minor quartzite, gabbro, and serpentinized ultramafic rocks (Fig. 2b–d and g–j). Clasts are angular to well rounded, poorly sorted, and matrix- or clast-supported. Gravel and pebble clasts are typically 2–20 cm in size, with rare boulders up to 1 m in size or even larger. The large size of clasts, combined with the textural immaturity of the conglomerate, indicates that the area of deposition was located near the source region.

Sandstone and mudstone, which are intercalated as thin layers or lenses within the conglomerate, form a subordinate lithofacies (Fig. 2a). Clastic grains in the sandstones are angular to subangular and poorly sorted, comprising lithic fragments (>80%), monocrystalline quartz (5%–20%), and rare feldspar and polycrystalline quartz (Fig. 2e–f). Lithic detritus consists of slate, siltstone, and radiolarian chert, with minor phyllite, basalt, and serpentinite.

Fig. 2. Petrographic features of the Liuqu Conglomerate. a, Sandstone bed within thick-bedded coarse conglomerate in the Liuqu section. Note the blocky shape of some clasts and the unsorted character of the conglomerate; b, outcrop in the Liuqu section containing rounded to subrounded, poorly sorted gravel dominated by quartz-arenite; c, outcrop in the Liuqu section containing blocky clasts of slate and litharenite; d, conglomerate in the Xialu section containing gravel-sized clasts of basalt, radiolarian chert, and gabbro; e, photomicrograph of sandstone (sample LQ07) from the Liuqu section, with clasts dominated by radiolarian chert and slate; f, photomicrograph of sandstone (XL01) from the Xialu section, containing detritus derived from quartz, siltstone, phyllite, and slate; g, photomicrograph of quartz-arenite gravel from the Liuqu section (LQ01); h, litharenite gravel from the Liuqu section (LQ02); i, olivine basalt gravel from the Xialu section (XL-L06), which is strongly altered (chloritized); and j, radiolarian chert gravel from the Xialu section (XL-L05). Ls, lithic sandstone; Lv, volcanic clast; Ol, olivine; Pl, plagioclase; Qm, monocrystalline quartz; Qp, polycrystalline quartz; Qs, quartz-arenite; Rs, radiolarian chert.

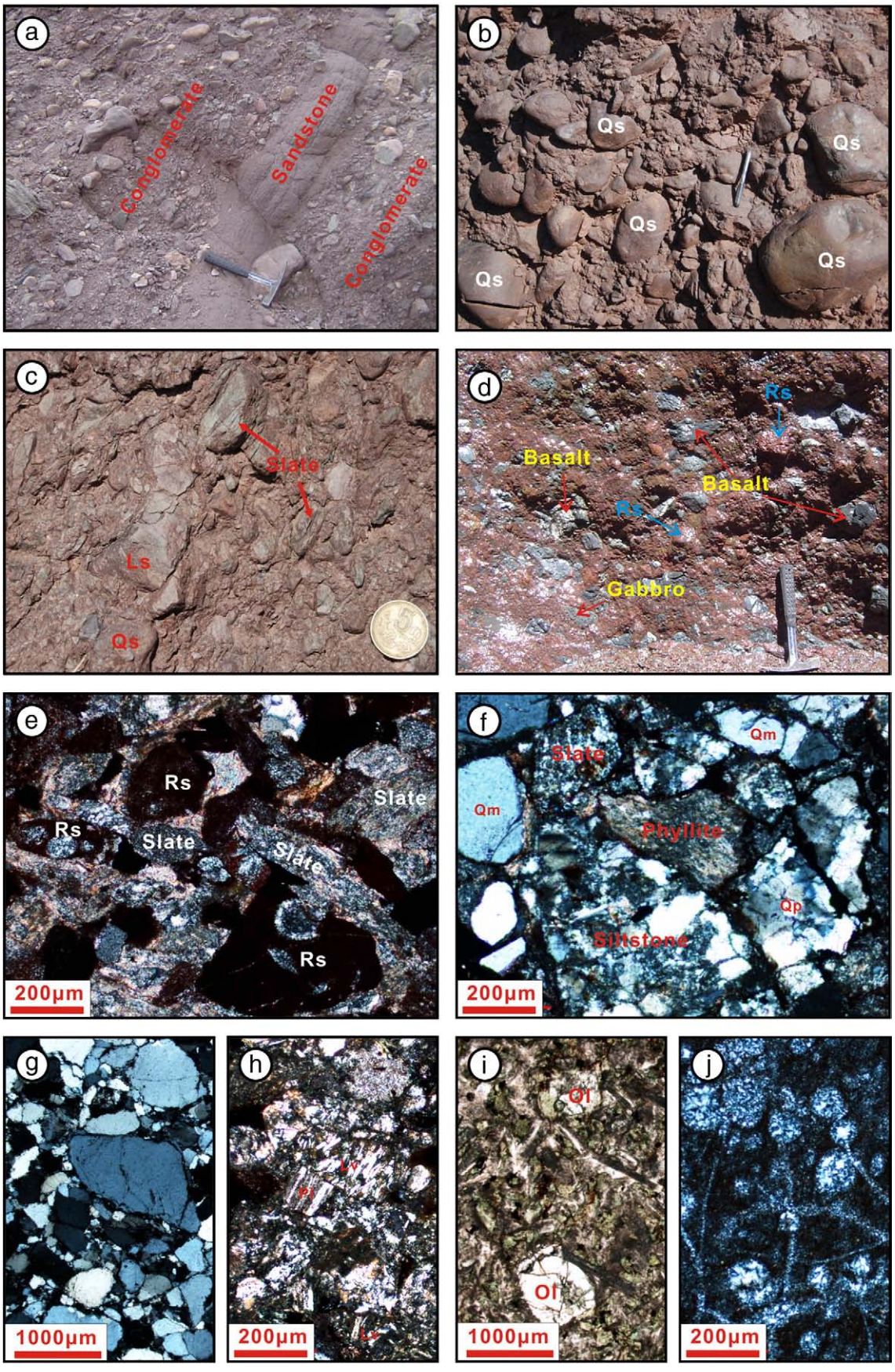

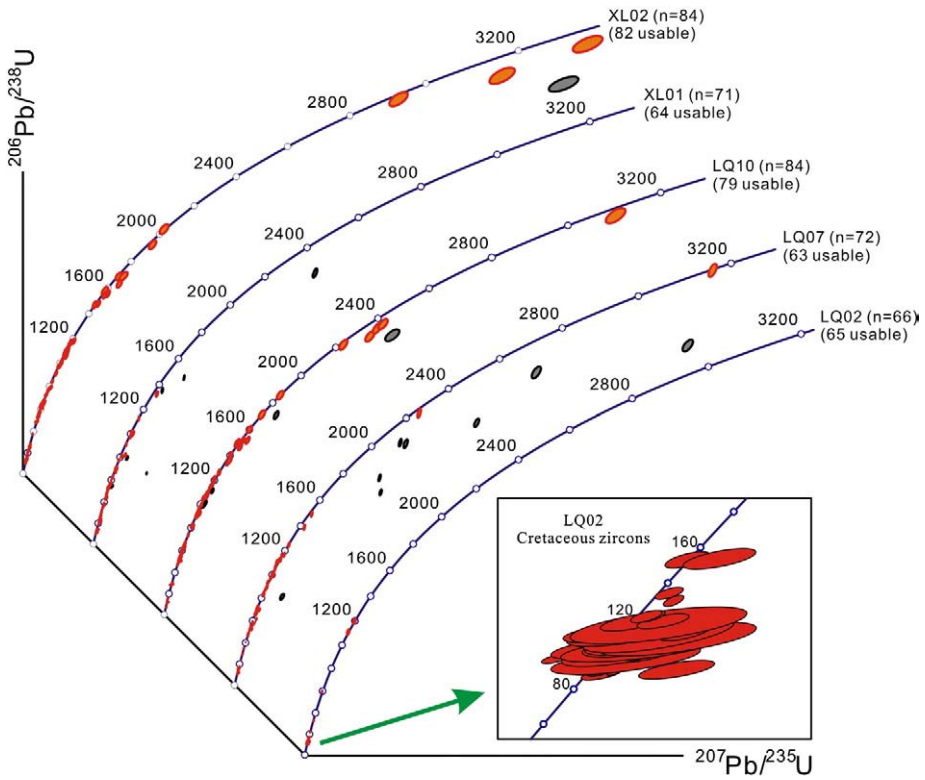

Fig. 3. U–Pb concordia for detrital zircon from the Liuqu Conglomerate. Ages are in Ma and ellipses show 1σ errors. Analyses in gray are highly discordant, and hence are not included in the discussion.

4.2. U–Pb geochronology of detrital zircon

From sample LQ07 (lower part of the Liuqu section), we randomly collected 72 detrital zircon grains for U–Pb dating. The CL images show that most zircons have well-developed oscillatory zoning, indicating a magmatic origin. A small number of zircons are of metamorphic origin, showing overgrowth rims or no zoning. Sixty-three ages were obtained with sufficient concordance and precision to provide provenance information (Fig. 3). Most of the ages plot within three distinct groups. The most prominent age peak occurs in the late Jurassic–Cretaceous (150–80 Ma), with lesser peaks in the Cambrian–Ordovician (540–450 Ma) and Meso–Neoproterozoic (1270–600 Ma) (Fig. 4a). In addition, four zircons yield Late Paleozoic to Early Mesozoic ages (217–391 Ma) and four yield ages of 1522 ± 10, 1569 ± 10, 2297 ± 10, and 3170 ± 10 Ma. The youngest ages, from sample LQ07, are 80 ± 2 and 81 ± 1 Ma.

Zircons from sample LQ10, which was collected from the upper part of the Liuqu section, are dominantly magmatic zircons with well-developed oscillatory zoning or sector zoning. Eighty-four analyses yielded 79 usable ages (Fig. 3). The age spectrum is similar to that obtained from LQ07, although Late Jurassic–Cretaceous zircons are relatively rare (only four grains), and two additional small peaks are found at ~1450 and ~2450 Ma (Fig. 4b). The analyses yielded one Paleocene age of 58 ± 1 Ma and other young ages of 92 ± 1 and 99 ± 1 Ma.

Samples XL01 and XL02, collected from the lower and upper parts of the Liuqu Conglomerate, respectively, at the Xialu locality, provided 64 and 82 ages of sufficient concordance and precision for provenance interpretation (Fig. 3). The CL images of most zircon grains show oscillatory compositional zoning, with a few homogeneous grains and some with core–rim structures. Most of the zircon ages plot into three clusters: Jurassic–Cretaceous (195–79 Ma), Cambrian–Ordovician (~540–470 Ma), and Meso–Neoproterozoic (~600–1250 Ma), similar to zircons from the Liuqu section. Only the Late Paleozoic–Early Mesozoic zircons are more common than in the Liuqu section, defining an age peak at ~400–200 Ma (Fig. 4c–d). The youngest ages determined from XL01 are 87 ± 2 and 91 ± 2 Ma, while those from XL02 are 79 ± 2, 83 ± 2, and 87 ± 2 Ma.

Sample LQ02, a litharenitic gravel from the Liuqu locality, yielded 65 credible ages from 66 analyses. Except for three Precambrian ages (581 ± 7, 1102 ± 14, and 1192 ± 15 Ma) and one Late Triassic age (209 ± 3 Ma), the remaining 61 zircon ages define a cluster at the Late Jurassic–early Late Cretaceous (153–88 Ma), with a peak age at ~104 Ma (Fig. 4e).

Collectively, sandstone samples from the Liuqu Conglomerate have similar detrital zircon ages, being mainly Late Jurassic–Cretaceous (~80–150 Ma) and Ordovician–Precambrian (mainly occur at ~450–1250 Ma) with minor Late Paleozoic–Early Mesozoic ages. Paleozoic and Mesozoic zircons are more abundant in samples from the Xialu section than in those from the Liuqu section. The age of the youngest grain is similar in all samples (~80 Ma), except in sample LQ10 which yields a Paleogene youngest age.

4.3. Hf isotopes in detrital zircon

We found a large population of grains aged ~80–150 Ma, with positive $\varepsilon_{Hf}(t)$ values between 0 and +16.7 and with two-stage Hf model ages (T^C_{DM}) of ~0.1–1.2 Ga. The well-developed oscillatory compositional zoning and positive $\varepsilon_{Hf}(t)$ values of these zircons indicate they were derived from a very juvenile magma source. We also found many magmatic zircons with ages of ca 110–140 Ma and with negative $\varepsilon_{Hf}(t)$ values from −1.0 to −17.0. The T^C_{DM} ages of these zircons show a wide range, from 1.2 to 2.3 Ga, suggesting a mixed magmatic source.

Three latest Triassic–Early Jurassic zircons with negative $\varepsilon_{Hf}(t)$ values form a small group on the $\varepsilon_{Hf}(t)$ vs age diagram (Fig. 5). Their $\varepsilon_{Hf}(t)$ values range from −13.2 to −8.9, and T^C_{DM} values are 1.8–2.1 Ga, indicating derivation from Paleoproterozoic crust. Early Mesozoic–Late Paleozoic (~200–400 Ma) zircons have a wide range of $\varepsilon_{Hf}(t)$ values, from −4.3 to +9.1; T^C_{DM} values range from 0.7 to 1.6 Ga.

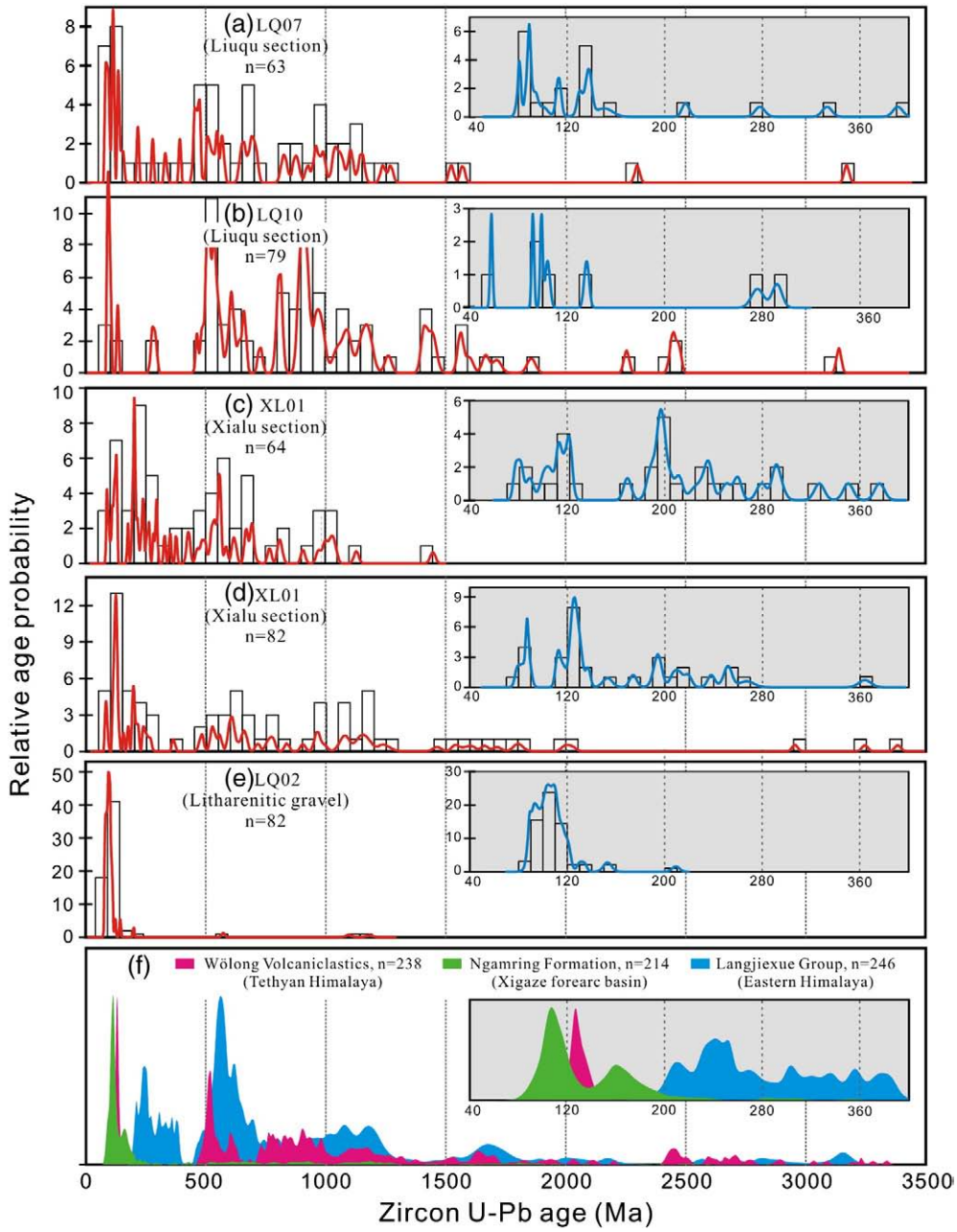

Fig. 4. Relative U–Pb age probability for detrital zircon from the Liuqu Conglomerate. Also shown for comparison are data from the Lower Cretaceous Wölong Volcaniclastics in the Tethyan Himalaya (Hu et al., 2010), Xigaze forearc basin (Wu et al., 2010), and the Langjiexue Group (Aikman et al., 2008).

Ordovician–Precambrian zircons (>450 Ma) are abundant, most of which have negative $\varepsilon_{Hf}(t)$ values. On the $\varepsilon_{Hf}(t)$ vs age diagram (Fig. 5), these zircons are distributed along a crustal evolution belt, with two-stage Hf model ages of ~1.5–3.0 Ga. These data suggest that the host magmas of these zircons were derived from similar Archean–Paleoproterozoic crustal materials.

5. Provenance of the Liuqu Conglomerate

5.1. Overview of zircon U–Pb ages and Hf isotope data from potential source regions

Zircon U–Pb ages and Hf isotopic data from neighboring terranes of the Yarlung-Zangbo suture zone are summarized to constrain the sources of the Liuqu Conglomerate (Table 1; Fig. 4f).

Detailed geochronologic studies indicate that Gangdese arc magmatism was active during the latest Triassic to Eocene (~200–40 Ma) (Chu et al., 2006; Wen et al., 2008; Ji et al., 2009). Zircons from Gangdese batholiths are characterized by positive $\varepsilon_{Hf}(t)$ values and two-stage Hf model ages (T^{C}_{DM}) from 0.3 to 1.0 Ga (Chu et al., 2006; Ji et al., 2009). In contrast, zircon from the Early Cretaceous granites of the north magmatic belt of the Lhasa terrane have negative $\varepsilon_{Hf}(t)$ values and T^{C}_{DM} values ranging from 1.4 to 2.1 Ga (Chu et al., 2006; Guynn et al., 2006). Jurassic and pre-Mesozoic inherited zircons and detrital zircons are common in northern Lhasa, showing dominantly negative $\varepsilon_{Hf}(t)$ values with T^{C}_{DM} ages ranging from 1.0 to 2.3 Ga (Chu et al., 2006; Leier et al., 2007). The Linzizong volcanic successions, which were erupted at ~65–43 Ma, contain zircons characterized by positive $\varepsilon_{Hf}(t)$ values, yielding T^{C}_{DM} ages of ~0.4 to ~1.1 Ga (Mo et al., 2008; Lee et al., 2009).

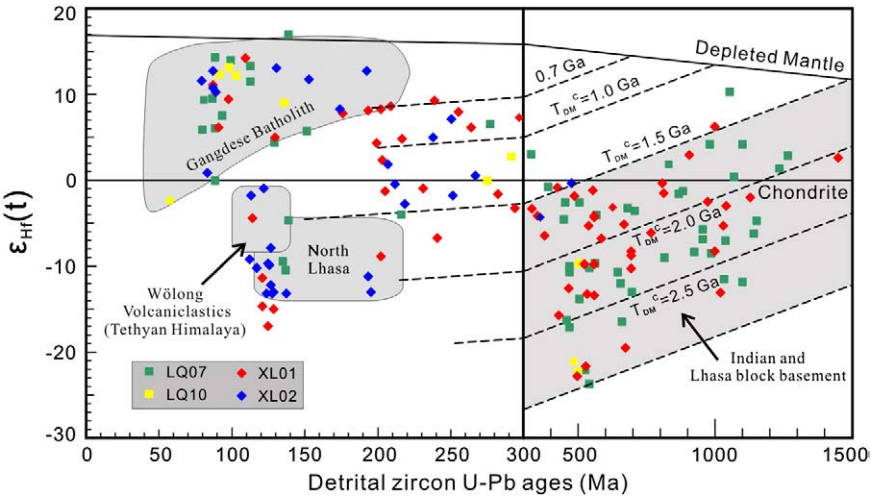

Fig. 5. Plots of $\varepsilon_{Hf}(t)$ values vs the U–Pb age of detrital zircon from sandstones within the Liuqu Conglomerate. Shading shows different fields corresponding to potential sources. Data sources are listed in Table 1.

Detrital zircons from the Xigaze forearc basin are mainly Jurassic–Cretaceous in age (>77 Ma), although some pre-Mesozoic grains are found (Fig. 4f), derived from the Lhasa terrane. Most of the Mesozoic zircons have positive $\varepsilon_{Hf}(t)$ values; a few zircons with negative $\varepsilon_{Hf}(t)$ values are found in the upper part of the forearc strata (Wu et al., 2010).

The Tethyan Himalaya lies south of the Yarlung-Zangbo suture zone. Detrital zircons from the clastic strata are Ordovician–Precambrian in age, with age peaks at ~450–550, ~570–1200, and ~1500 Ma (Gehrels et al., 2003, 2006; Myrow et al., 2003). The Lower Cretaceous strata (e.g., the Wölong Volcaniclastics at Tingri) contain an additional cluster of Early Cretaceous zircons (~145–120 Ma) with negative $\varepsilon_{Hf}(t)$ values (−1.5 to −7.2) (Hu et al., 2008, 2010) (Fig. 4f). In the eastern Himalaya, the Triassic Langjiexue Group shows different detrital zircon age patterns to those obtained from Tethyan Himalaya sediments. In addition to Precambrian–Ordovician zircons, which are common in the Tethyan Himalayas, abundant Late Paleozoic to Early Mesozoic (~200–400 Ma) zircons define distinct age peaks (Fig. 4f) (Aikman et al., 2008).

Aitchison et al. (2000) proposed the presence of a remnant intra-oceanic arc along the Yarlung-Zangbo suture zone in the Zedong area. Geochronologic studies indicate that the intra-oceanic arc would have been active during the late Middle Jurassic–mid Late Jurassic (161–152 Ma) (McDermid et al., 2002; Aitchison et al., 2007b); however, isotopic data are lacking.

5.2. Provenance interpretations

The proposed provenance of the Liuqu Conglomerate is based on a comparison of clast composition, zircon age patterns, and Hf isotopes between the conglomerate and potential source rocks in the regions surrounding the Yarlung-Zangbo suture zone (Figs. 4 and 5).

The coarse-grained and immature texture of the Liuqu Conglomerate indicates that clasts were derived from proximal sources. Clasts of basalt, gabbro, serpentinized ultramafic rocks, and radiolarian chert were unequivocally derived from an ophiolitic source (Davis et al., 2002). The conglomerate is in depositional contact with or located immediately south of the Yarlung-Zangbo ophiolite, indicating that the ophiolite is the most likely source for such clasts. Other ophiolitic rocks, such as the Bangong-Nujiang ophiolite, are located far from the Liuqu Conglomerate, making it highly unlikely that they were the source rocks. Quartz-arenites, slate, and phyllite are typical components of the north Indian passive margin, which lies immediately south of the Liuqu Conglomerate, thereby providing a source for the conglomerate (Davis et al., 2002). The provenance of the litharenitic gravel is difficult to determine because this rock type is present in all of the neighboring terranes.

Zircons of 80–150 Ma in age can be subdivided into one group with positive $\varepsilon_{Hf}(t)$ values and another with negative $\varepsilon_{Hf}(t)$ values (Fig. 5). The grains with negative $\varepsilon_{Hf}(t)$ values were possibly derived from Cretaceous strata of the Tethyan Himalaya or from the north Lhasa terrane of the Asian plate. Grains with positive $\varepsilon_{Hf}(t)$ values were derived from the Asian plate, from the Gangdese magmatic arc, as no suitable source has yet been identified on the Indian margin (Table 1). However, Gangdese magmatism was active during the Late Triassic to Eocene (~200–40 Ma) (Chung et al., 2005; Wen et al., 2008; Ji et al., 2009; Lee et al., 2009), whereas latest Cretaceous and Paleogene zircons are almost absent in the Liuqu Conglomerate (the youngest age population is at ~80 Ma, with only one age of 58 Ma) (Fig. 4). This contradiction could be interpreted in two ways: (1) younger grains from the Gangdese batholith are absent from the Liuqu Conglomerate because of slow exhumation from depth, or (2) the zircons were not

Table 1
Zircon U–Pb age data and Hf isotope data from potential sources for the Liuqu Conglomerate.

Potential sources	Ages/Ma	$\varepsilon_{Hf}(t)$	T_{DM}^{C}/Ga	References
North Lhasa terrane	~120–210	0 to −14	1.4–2.1	Chu et al. (2006)
	>500	−20 to +11	1.0–2.3	Guynn et al. (2006), Leier et al. (2007)
Gangdese batholith	~40–200	0 to +17	0.3–1.0	Chu et al. (2006), Ji et al. (2009)
Linzizong volcanic successions	~65–43 Ma	+0.5 to +11	0.4–1.1	Mo et al. (2008), Lee et al. (2009)
Xigaze forearc sequence	80–200 (major)	Positive (major, to +16)	0.1–1.2	Wu et al. (2010)
		Negative (minor, to −18)	1.2–2.3	
	>450 (minor)	−20 to +10	1.0–3.7	
Intra-oceanic arc	~161–152	Lack	Lack	McDermid et al. (2002), Aitchison et al. (2007b)
Langjiexue Group	200–400	Lack	Lack	Aikman et al. (2008)
	>450	Lack	Lack	
Tethyan sequence	~120–140	−1.5 to −7.2	1.3–1.6	Gehrels et al. (2003, 2006), Hu et al. (2010)
	>450	−12.5 to +6.4	1.5–3.7	

derived directly from the Gangdese arc, but were recycled from the Xigaze forearc sequences. The first interpretation is unlikely because one might expect to see young zircons from the Linzizong volcanic successions, since they were erupted at the surface and are widespread in the southern Lhasa terrane. We prefer the latter explanation because (1) the Xigaze forearc sediments were derived from the Lhasa terrane and contain abundant Gangdese zircons older than 77 Ma (Wu et al., 2010); (2) the ages of zircon grains from a litharenitic gravel within the Liuqu Conglomerate define a cluster at 153–88 Ma, identical to the zircon ages from the lower part of the Xigaze Group (Fig. 4) (Wu et al., 2010); and (3) our field investigations, as well as those of Davis et al. (2002), revealed no Gangdese-derived clasts (e.g., rhyolite, andesite, and volcaniclastics) in the Liuqu Conglomerate. Late Triassic–Early Jurassic zircons with negative $\varepsilon_{Hf}(t)$ values could also have been recycled from the Xigaze Group, since such zircons are present in the upper part of the Xigaze forearc successions. Therefore, we conclude that at least some of the litharenite clasts in the Liuqu Conglomerate, if not all, were derived from the Xigaze forearc basin of the Asian plate. This conclusion is in contrast with that made by Davis et al. (2002), who suggested that these clasts were derived from an intra-oceanic arc and that no detritus in the Liuqu Conglomerate is derived from terranes to the north of the Yarlung-Zangbo suture.

Zircon grains with ages of ~200–400 Ma are considered to have been derived from the Triassic Langjiexue Group, since zircons of such age are not known from the Xigaze forearc deposits, or the Tethyan Himalaya, apart from the Langjiexue Group (Aikman et al., 2008). The only unsatisfactory issue is that the Langjiexue Group occurs east of Lhasa City, being far from the area in which the conglomerate was deposited (Fig. 1). Several hypotheses can be invoked to explain the problem of proximal depositional characteristics but large present-day distance from the source to the depositional area: (1) the Langjiexue Group was originally much larger than its present-day extent, but was partly subducted or eroded during tectonic shortening following India–Asia collision; (2) equivalent deposits of the Langjiexue Group may exist west of Lhasa, but have yet to be found; (3) large-scale strike-slip displacement may have occurred along the Yarlung-Zangbo suture zone; and (4) these grains were derived from unknown sources other than the Langjiexue Group.

Ordovician–Precambrian (>450 Ma) zircon grains are common in the Tethyan Himalaya. Even so, similarly old grains are found in other neighboring terranes. Based on this observation, in combination with the previous discussion, we speculate that these zircons have multiple sources, including the Tethyan sequences, Xigaze forearc deposits, and the Langjiexue Group.

Contrary to previous interpretations (Aitchison et al., 2000; Davis et al., 2002), our results indicate that Asian material is found within the Liuqu Conglomerate, thereby indicating that the conglomerate is a post-collisional molasse that records erosion from both the Indian and Asian margins. It remains uncertain whether material from an intra-oceanic arc was incorporated into the Liuqu Conglomerate. Remnant intra-oceanic arc is restricted to the Zedong area, and little is known regarding its lithologic and isotopic characteristics. Consequently, it is difficult to determine, based on petrographic and isotopic comparisons, if clasts within the conglomerate were derived from this arc. However, andesite and dacite reported from the arc (Aitchison et al., 2000) are not observed in the Liuqu Conglomerate. The arc was active during the period 161–152 Ma (McDermid et al., 2002; Aitchison et al., 2007b); however, zircons of this age are scarce in the Liuqu Conglomerate.

6. Discussion

6.1. Depositional model for the Liuqu Conglomerate

As outlined in the Introduction, two different geotectonic models have been proposed to explain the deposition of the Liuqu Conglomerate. One of the models considers that the conglomerate represents molasse deposited after India–Asia collision, when the Yarlung-Zangbo suture zone underwent rapid uplift and erosion due to ongoing crustal thickening (e.g., Yin et al., 1988; Einsele et al., 1994). It has been suggested that clasts within the Liuqu Conglomerate were derived locally from the Xigaze forearc basin and the Yarlung-Zangbo ophiolite, and accumulated in a sedimentary basin formed to the south of the uplifted highland. The other model states that the Liuqu Conglomerate represents the accumulation of clastic rocks during collision between India and an intra-oceanic arc, predating the final India–Asia collision (Aitchison et al., 2000; Davis et al., 2002). The second model is inconsistent with the provenance data presented here, which demonstrate that Asian-derived (Xigaze forearc basin) detritus is present in the Liuqu Conglomerate, indicating that deposition occurred after India–Asia continental collision.

The present isotopic data support the first model to some degree, despite the fact that the data suggest a relatively complex provenance for the Liuqu Conglomerate. In combining our new provenance data with the results of previous studies (Yin et al., 1988; Davis et al., 2002; Fang et al., 2006), we suggest that the deposition of the Liuqu Conglomerate occurred in association with uplift of the Yarlung-Zangbo suture zone during the Middle–Late Eocene (Fig. 6). The uplifted landscape along the suture at this time, which may have included collision-related mélange, the Xigaze forearc basin, and the Yarlung-Zangbo ophiolite, would have been eroded, providing coarse-grained clastic debris to streams and rivers, leading to the development of alluvial fans and deltas upon basin floors, which were elongate and oriented parallel to the southern front of the range. The uplifted highland would have acted as a barrier, preventing the Gangdese detritus from being transported farther south, thereby explaining the absence of Gangdese-derived clasts in the Liuqu Conglomerate. This model suggests that the Liuqu Conglomerate was originally mainly deposited south of the suture, which is in agreement with its present-day distribution (Pan and Ding, 2004). It is notable that Liuqu Conglomerate occurs in a few places north of the Yarlung-Zangbo ophiolite, but is in fault contact with underlying rocks (Davis et al., 2002; Pan and Ding, 2004). We attribute that the development of Tertiary north-dipping Himalayan thrusts and the south-dipping Great Counter Thrust system (GCT) (Quidelleur et al., 1997; Yin et al., 1999) may carry the Liuqu Conglomerate north to the ophiolite.

6.2. Implications for the Himalayan–Tibetan orogen

The genetic link between orogenic belts and synorogenic sediments has long been recognized and exploited in studies of orogenic history, in a variety of tectonic setting (e.g., DeCelles et al., 1991; DeCelles, 1994; Dávila and Astini, 2007). Synorogenic conglomerates are particularly useful in studies of the timing and erosion history of orogenesis.

The presence of Asian-derived clasts in the Liuqu Conglomerate indicates that the conglomerate was deposited after India–Asia collision, thereby providing an additional constraint on the timing of continental collision. Although the depositional age of the conglomerate is not well constrained, sedimentation started during the Middle Eocene (Tao, 1988; Fang et al., 2006).

Deposition of the Liuqu Conglomerate occurred mainly on alluvial fans and in braided river systems (Davis et al., 2002), indicating that the proximal source areas were areas of considerable relief. Thus, the present findings suggest that the Liuqu Conglomerate records a period of erosion of the Himalayan–Tibet orogen during the Middle–Late Eocene, which provides an age constraint for the onset of orogenic erosion in the east-central Himalaya. The proposed timing of erosion of the Himalayan–Tibetan orogen is supported by the age of sedimentary deposits within the Indus-Yarlung-Zangbo suture zone and remnant oceanic basins. In the Indus suture zone, the age of the Indus Group molasse, which comprises detritus predominantly from

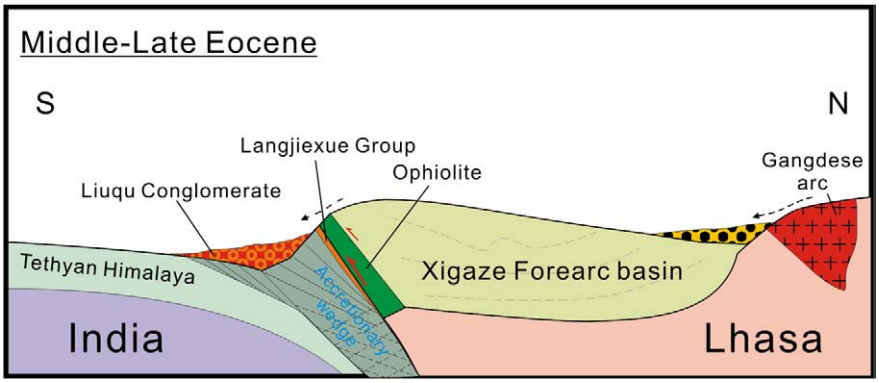

Fig. 6. Tectonic–depositional model for the Liuqu Conglomerate, modified after Yin et al. (1988).

the Asian Trans-Himalaya to the north and subordinately from the Indian crust to the south (Clift et al., 2002; Wu et al., 2007), is constrained by Early Eocene Chogdo Formation (Sinclair and Jaffey, 2001). In the Indus fan, detritus eroded from the Himalaya first appears in Middle Eocene strata (Clift et al., 2001). Similarly, in the Bengal basin, the first orogeny-related material arrived between 50 and 38 Ma, while a substantial input of detritus from the metamorphosed Himalaya occurred at 38 Ma (Najman et al., 2008). Thus, a broad range of regional data demonstrates that the inception of erosion of the Himalayan–Tibetan orogen occurred as early as the Early Eocene. In the Himalaya foreland basin, the substantial input of Himalayan detritus is first observed above the basin-wide unconformity, in alluvial facies younger than 36 Ma in Pakistan (Najman et al., 2001) and younger than 31 Ma in India (Najman et al., 2004). The depositional age of these sediments is significantly younger than the age of onset of Himalaya erosion, possibly suggesting a progressive southward shift of the main thrust after India–Asia collision.

Various geodynamic mechanisms have been proposed for synorogenic conglomerate, including thrust propagation and isostatic uplift (e.g., DeCelles, 1994; DeCelles et al., 1991; Sinclair, 1997; Dávila and Astini, 2007). We speculate that isostatic uplift induced by Neotethyan slab breakoff was the most likely control on deposition of the Liuqu Conglomerate. Neotethyan slab breakoff is thought to have occurred at ~50–45 Ma, as indicated by Eocene Himalayan metamorphism (Ding et al., 2001; Kohn and Parkinson, 2002), a flare-up (at ~50 Ma) and subsequent cessation of Linzizong volcanism (Lee et al., 2009), emplacement of intraplate-type mafic dykes (40–42 Ma, Xu et al., 2008), onset of the rapid cooling of Gangdese batholiths (~42 Ma, He et al., 2007), and exhumation of ultrahigh-pressure rocks (Leech et al., 2005). The similarity in the timing of events related to slab breakoff and the depositional of the Liuqu Conglomerate suggests a possible link. With slab breakoff, removal of the load of the subducting slab would have generated rapid isostatic uplift, leading to rapid erosion of the Himalayan–Tibetan orogen.

7. Concluding remarks

The Liuqu Conglomerate consists of granule- to boulder-sized clastics with minor intercalated sandstones and mudstones. The strata were deposited mainly on alluvial fans and in braided river systems, with a cumulative thickness at the Liuqu locality in excess of 3500 m. The unsorted to poorly sorted character of the sediments, together with the occurrence of boulders up to 1 m in size, indicates that the area of deposition was located very close to the source areas. Clasts in the conglomerate consist of quartz-arenite, litharenite, slate, radiolarian chert, and basalt, along with minor phyllite, gabbro, and serpentinite. Radiolarian chert, and mafic and ultramafic detritus are clearly derived from the Yarlung-Zangbo suture ophiolite.

We improved upon previous studies of the source of the Liuqu Conglomerate by analyzing U–Pb and Hf isotopes of detrital zircons. Detrital zircon ages are concentrated in three clusters at 80–150, 200–400, and ~450–1250 Ma. Zircons of 80–150 Ma in age can be subdivided into two groups: a group with positive $\varepsilon_{Hf}(t)$ values shows a Gangdese affinity and is considered to have been recycled from sedimentary strata of the Xigaze forearc basin, while a group with negative $\varepsilon_{Hf}(t)$ values was derived either from Cretaceous strata of the Tethyan Himalaya or from the north Lhasa terrane of the Asian plate. Zircons with ages of 200–400 Ma and $\varepsilon_{Hf}(t)$ values of −4.3 to +9.1 were derived from Triassic clastic rocks of the Langjiexue Group, as this is the only possible source, to the best of our knowledge. Zircons older than 450 Ma may have multiple sources, including Tethyan sequences, the Langjiexue Group, and even the Xigaze forearc sediments.

The occurrence of Asian-derived detritus in the Liuqu Conglomerate, deposited above the Indian plate and ophiolite, indicates that the conglomerate is a post-collisional molasse that records the early erosion of the Himalayan–Tibetan orogen. The similarity in the timing of events related to slab breakoff and the depositional of the Liuqu Conglomerate suggest a possible link. With slab breakoff, removal of the load of the subducting slab would have generated rapid isostatic uplift, leading to rapid erosion of the Himalayan–Tibetan orogen.

Supplementary materials related to this article can be found online at doi:10.1016/j.sedgeo.2010.09.004.

Acknowledgements

This work was financially supported by the MOST 973 Project (2006CB701402) and an NSFC Grant (40772070). We thank Xiang Li for help in the field, Zhi-Cheng Huang for assistance in analyzing thin sections, and Xi-Sheng Xu and Bin Wu for help with zircon analyses. We are grateful to Profs. Cheng-Shan Wang, Xiang-Hui Li, and Di-Cheng Zhu for valuable discussions and suggestions. The manuscript benefited from careful reviews and advice from Yani Najman and an anonymous reviewer.

References

Aikman, A.B., Harrison, T.M., Lin, D., 2008. Evidence for Early (>44 Ma) Himalayan Crustal Thickening, Tethyan Himalaya, southeastern Tibet. Earth and Planetary Science Letters 274 (1–2), 14–23.

Aitchison, J.C., Ba, D.Z., Davis, A.M., Liu, J.B., Luo, H., Malpas, J.G., McDermid, I.R.C., Wu, H.Y., Ziabrev, S.V., Zhou, M.F., 2000. Remnants of a Cretaceous intra-oceanic subduction system within the Yarlung-Zangbo suture (southern Tibet). Earth and Planetary Science Letters 183 (1–2), 231–244.

Aitchison, J.C., Davis, A.M., Zhu, B., Luo, H., 2002. New constraints on the India–Asia collision: the lower Miocene Gangrinboche Conglomerates, Yarlung Tsangpo suture zone, SE Tibet. Journal of Asian Earth Sciences 21 (3), 251–263.

Aitchison, J.C., Ali, J.R., Davis, A.M., 2007a. When and where did India and Asia collide? Journal of Geophysical Research 112, B05423. doi:10.1029/2006JB004706.

Aitchison, J.C., McDermid, I.R.C., Ali, J.R., Davis, A.M., Zyabrev, S.V., 2007b. Shoshonites in southern Tibet record Late Jurassic rifting of a Tethyan intra-oceanic island arc. Journal of Geology 115 (2), 197–213.

BlichertToft, J., Albarede, F., 1997. The Lu–Hf isotope geochemistry of chondrites and the evolution of the mantle–crust system. Earth and Planetary Science Letters 148 (1–2), 243–258.

Burbank, D.W., Beck, R.A., Mulder, T., 1996. In: Yin, A., Harrison, T.M. (Eds.), The Himalayan Foreland Basin: the Tectonic Evolution of Asia. Cambridge University Press, pp. 149–188.

Chu, M.F., Chung, S.L., Song, B.A., Liu, D.Y., O'Reilly, S.Y., Pearson, N.J., Ji, J.Q., Wen, D.J., 2006. Zircon U–Pb and Hf isotope constraints on the Mesozoic tectonics and crustal evolution of southern Tibet. Geology 34 (9), 745–748.

Chung, S.L., Chu, M.F., Zhang, Y.Q., Xie, Y.W., Lo, C.H., Lee, T.Y., Lan, C.Y., Li, X.H., Zhang, Q., Wang, Y.Z., 2005. Tibetan tectonic evolution inferred from spatial and temporal variations in post-collisional magmatism. Earth-Science Reviews 68 (3–4), 173–196.

Clift, P.D., Shimizu, N., Layne, G.D., Blusztajn, J.S., Gaedicke, C., Schluter, H.U., Clark, M.K., Amjad, S., 2001. Development of the Indus Fan and its significance for the erosional history of the Western Himalaya and Karakoram. Geological Society of America Bulletin 113, 1039–1051.

Clift, P.D., Carter, A., Krol, M., Kirby, E., 2002. Constraints on India–Eurasia collision in the Arabian Sea region taken from the Indus Group, Ladakh Himalaya, India. Geological Society, London, Special Publications 195, 97–116.

Dai, J., Yin, A., Liu, W., Wang, C., 2008. Nd isotopic compositions of the Tethyan Sequence in southeastern Tibet. Science in China, Series D: Earth Sciences 51 (9), 1306–1316.

Dávila, F.M., Astini, R.A., 2007. Cenozoic provenance history of synorogenic conglomerates in western Argentina (Famatina belt): implications for Central Andean foreland development. Geological Society of America Bulletin 119, 609–622.

Davis, A.M., Aitchison, J.C., Ba, D.Z., Luo, H., Zyabrev, S., 2002. Paleogene island arc collision-related conglomerates, Yarlung-Tsangpo suture zone, Tibet. Sedimentary Geology 150 (3–4), 247–273.

DeCelles, P.G., Gray, M.B., Ridgway, K.D., Cole, R.B., Srivastava, P., Pequera, N., Pivnik, D.A., 1991. Kinematic history of a foreland uplift from Paleocene synorogenic conglomerate, Beartooth Range, Wyoming and Montana. Geological Society of America Bulletin 103, 1458–1475.

DeCelles, P.G., 1994. Late Cretaceous–Paleocene synorogenic sedimentation and kinematic history of the Sevier thrust belt, northeast Utah and southwest Wyoming. Geological Society of America Bulletin 106, 32–56.

Ding, L., Zhong, D.L., Yin, A., Kapp, P., Harrison, T.M., 2001. Cenozoic structural and metamorphic evolution of the eastern Himalayan syntaxis (Namche Barwa). Earth and Planetary Science Letters 192, 423–438.

Ding, L., Kapp, P., Wan, X.Q., 2005. Paleocene–Eocene record of ophiolite obduction and initial India–Asia collision, south central Tibet. Tectonics 24 (3), 1–18.

Dubois-Coté, V., Hébert, R., Dupuis, C., Wang, C.S., Li, Y.L., Dostal, J., 2005. Petrological and geochemical evidence for the origin of the Yarlung Zangbo ophiolites, southern Tibet. Chemical Geology 214, 265–286.

Dürr, S.B., 1996. Provenance of Xigaze fore-arc basin clastic rocks (Cretaceous, South Tibet). Geological Society of America Bulletin 108 (6), 669–684.

Einsele, G., Liu, B., Duerr, S., Frisch, W., Liu, G., Luterbacher, H.P., Ratschbacher, L., Richen, W., Wendt, J., Wetzel, A., Yu, G., Zheng, H., 1994. The Xigaze forearc basin: evolution and facies architecture (Cretaceous, Tibet). Sedimentary Geology 90 (1–2), 1–32.

Fang, A.M., Yan, Z., Liu, X.H., Pan, Y.S., Li, J.L., Yu, L.J., Huang, F.X., Tao, J.R., 2006. The age of the plant fossil assemblage in the Liuqu Conglomerate of southern Tibet and its tectonic significance. Progress in Natural Science 16 (1), 55–64.

Garzanti, E., 1999. Stratigraphy and sedimentary history of the Nepal Tethys Himalaya passive margin. Journal of Asian Earth Sciences 17 (5–6), 805–827.

Gehrels, G.E., DeCelles, P.G., Martin, A., Ojha, T.P., Pinhassi, G., Upreti, B.N., 2003. Initiation of the Himalayan Orogen as an early Paleozoic thin-skinned thrust belt. Geological Society of America Today 13 (9), 4–9.

Gehrels, G.E., DeCelles, P.G., Ojha, T.P., Upreti, B.N., 2006. Geologic and U–Pb geochronologic evidence for early Paleozoic tectonism in the Dadeldhura thrust sheet, far-west Nepal Himalaya. Journal of Asian Earth Sciences 28 (4–6), 385–408.

Griffin, W.L., Pearson, N.J., Belousova, E., Jackson, S.E., van Achterbergh, E., O'Reilly, S.Y., Shee, S.R., 2000. The Hf isotope composition of cratonic mantle: LAM–MC–ICPMS analysis of zircon megacrysts in kimberlites. Geochimica Et Cosmochimica Acta 64 (1), 133–147.

Griffin, W.L., Wang, X., Jackson, S.E., O'Reilly, S.Y., Xu, X.S., Zhou, X.M., 2002. Zircon chemistry and magma mixing, SE China: *in-situ* analysis of Hf isotopes, Tonglu and Pingtan igneous complexes. Lithos 61 (3–4), 237–269.

Guynn, J.H., Kapp, P., Pullen, A., Heizler, M., Gehrels, G., Ding, L., 2006. Tibetan basement rocks near Amdo reveal 'missing' Mesozoic tectonism along the Bangong suture, central Tibet. Geology 34 (6), 505–508.

Harrison, T.M., Copeland, P., Hall, S.A., Quade, J., Burner, S., Ohja, T.P., Kidd, W.S.F., 1993. Isotopic preservation of Himalayan/Tibetan uplift, denudation, and climate histories of two molasse deposits. Journal of Geology 100, 157–175.

He, S., Kapp, P., DeCelles, P.G., Gehrels, G.E., Heizler, M., 2007. Cretaceous–Tertiary geology of the Gangdese Arc in the Linzhou area, southern Tibet. Tectonophysics 433, 15–37.

Hodges, K.V., 2000. Tectonics of the Himalaya and southern Tibet from two perspectives. Geological Society of America Bulletin 112 (3), 324–350.

Hu, X., Jansa, L., Wang, C., 2008. Upper Jurassic–Lower Cretaceous stratigraphy in southeastern Tibet: comparison with the western Himalayas. Cretaceous Research 29, 301–315.

Hu, X.M., Jansa, L., Chen, L., Griffin, W.L., O'Reilly, S.Y., Wang, J.G., 2010. Provenance of lower cretaceous Wölong Volcaniclastics in the Tibetan Tethyan Himalaya: implications for the final break-up of Eastern Gondwana. Sedimentary Geology 223, 193–205.

Jackson, S.E., Pearson, N.J., Griffin, W.L., Belousova, E.A., 2004. The application of laser ablation–inductively coupled plasma–mass spectrometry to *in situ* U–Pb zircon geochronology. Chemical Geology 211 (1–2), 47–69.

Jadoul, F., Berra, F., Garzanti, E., 1998. The Tethys Himalayan passive margin from late Triassic to early Cretaceous (South Tibet). Journal of Asian Earth Sciences 16 (2–3), 173–194.

Ji, W.Q., Wu, F.Y., Chung, S.L., Li, J.X., Liu, C.Z., 2009. Zircon U–Pb geochronology and Hf isotopic constraints on petrogenesis of the Gangdese batholith, southern Tibet. Chemical Geology 262, 229–245.

Kohn, M.J., Parkinson, C.D., 2002. Petrologic case for Eocene slab breakoff during the Indo-Asian collision. Geology 30, 591–594.

Klootwijk, C.T., Gee, J.S., Peirce, J.W., Smith, G.M., MaFadden, P.L., 1992. An early India–Asia contact: paleomagnetic constraints from Ninetyeast Ridge, ODP Leg 121. Geology 20, 395–398.

Lee, H.Y., Chung, S.L., Wang, Y.B., Zhu, D.C., Yang, J.H., Song, B., Liu, D.Y., Wu, F.Y., 2007. Age, petrogenesis and geological significance of the Linzizong volcanic successions in the Linzhou basin, southern Tibet: evidence from zircon U–Pb dates and Hf isotopes. Acta Petrologica Sinica 23 (2), 493–500.

Lee, H.Y., Chung, S.L., Lo, C.H., Ji, J.Q., Lee, T.Y., Qian, Q., Zhang, Q., 2009. Eocene Neotethyan slab breakoff in southern Tibet inferred from the Linzizong volcanic record. Tectonophysics 477, 20–35.

Leech, M.L., Singh, S., Jain, A.K., Klemperer, S.L., Manickavasagam, R.M., 2005. The onset of India–Asia continental collision: early, steep subduction required by the timing of UHP metamorphism in the western Himalaya. Earth and Planetary Science Letters 234 (1–2), 83–97.

Leier, A.L., Kapp, P., Gehrels, G.E., DeCelles, P.G., 2007. Detrital zircon geochronology of Carboniferous–Cretaceous strata in the Lhasa Terrane, southern Tibet. Basin Research 19, 361–378.

Li, J.G., Guo, Z.Y., Batten, D.J., Cai, H.W., Zhang, Y.Y., 2010. Palynological stratigraphy of the Late Cretaceous and Cenozoic collision-related conglomerates at Qiabulin, Xigaze, Xizang (Tibet) and its bearing on palaeoenvironmental development. Journal of Asian Earth Sciences 38, 86–95.

Li, X.H., Zeng, Q.G., Wang, C.S., 2003. Paleocurrent data: evidence for the source of the Langjiexue Group in Southern Tibet. Geological Review 49 (3), 132–137 (in Chinese).

Liu, G.H., Einsele, G., 1994. Sedimentary history of the Tethyan basin in the Tibetan Himalayas. Geologische Rundschau 83 (1), 32–61.

McDermid, I.R.C., Aitchison, J.C., Davis, A.M., Harrison, T.M., Grove, M., 2002. The Zedong terrane: a Late Jurassic intra-oceanic magmatic arc within the Yarlung-Tsangpo suture zone, southeastern Tibet. Chemical Geology 187 (3–4), 267–277.

Mo, X.X., Niu, Y.L., Dong, G.C., Zhao, Z.D., Hou, Z.Q., Zhou, S., Ke, S., 2008. Contribution of syncollisional felsic magmatism to continental crust growth: a case study of the Paleogene Linzizong volcanic Succession in southern Tibet. Chemical Geology 250 (1–4), 49–67.

Myrow, P.M., Hughes, N.C., Paulsen, T.S., Williams, I.S., Parcha, S.K., Thompson, K.R., Bowring, S.A., Peng, S.C., Ahluwalia, A.D., 2003. Integrated tectonostratigraphic analysis of the Himalaya and implications for its tectonic reconstruction. Earth and Planetary Science Letters 212 (3–4), 433–441.

Najman, Y., 2006. The detrital record of orogenesis: a review of approaches and techniques used in the Himalayan sedimentary basins. Earth-Science Reviews 74 (1–2), 1–72.

Najman, Y., Garzanti, E., 2000. Reconstructing early Himalayan tectonic evolution and paleogeography from Tertiary foreland basin sedimentary rocks, northern India. Geological Society of America Bulletin 112, 435–449.

Najman, Y., Pringle, M., Godin, L., Oliver, G., 2001. Dating of the oldest continental sediments from the Himalayan foreland basin. Nature 410, 194–197.

Najman, Y., Johnson, C., White, N.M., Oliver, G., 2004. Evolution of the Himalayan foreland basin, NW India. Basin Research 16, 1–24.

Najman, Y., Bickle, M., BouDagher-Fadel, M., Carter, A., Garzanti, E., Paul, M., Wijbrans, J., Willett, E., Oliver, G., Parrish, R., Akhter, S.H., Allen, R., Ando, S., Chisty, E., Reisberg, L., Vezzoli, G., 2008. The Paleogene record of Himalayan erosion: Bengal Basin, Bangladesh. Earth and Planetary Science Letters 273 (1–2), 1–14.

Pan, G.T., Ding, J., 2004. Geological map (1:1500000) of Qinghai-Xizang (Tibetan) Plateau and adjacent areas. Chengdu: Chengdu Cartographic Publishing House, 1–133.

Quidelleur, X., Grove, M., Lovera, O.M., Harrison, T.M., Yin, A., Ryerson, F.J., 1997. Thermal evolution and slip history of the Renbu-Zedong thrust, southeastern Tibet. Journal of Geophysical Research 102, 2659–2679.

Rowley, D.B., 1996. Age of initiation of collision between India and Asia: a review of stratigraphic data. Earth and Planetary Science Letters 145 (1–4), 1–13.

Searle, M.P., Corfield, R.I., Stephenson, B., McCarron, J., 1997. Structure of the north India continental margin in the LadaKh–Zanskar Himalayas: implications for the timing of obduction of the Spontang ophiolite, India–Asia collision and deformation events in the Himalaya. Geological Magazine 134, 297–316.

Sinclair, H.D., 1997. Flysch to molasse transition in peripheral foreland basins: the role of the passive margin versus slab breakoff. Geology 25 (12), 1123–1126.

Sinclair, H.D., Jaffey, N., 2001. Sedimentology of the Indus Group, Ladakh, northern India: implications for the timing of initiation of the palaeo-Indus River. Journal of the Geological Society, London 158, 151–162.

Soederlund, U., Patchett, P.J., Vervoort, J.D., Isachsen, C.E., 2004. The ^{176}Lu decay constant determined by Lu–Hf and U–Pb isotope systematics of Precambrian mafic intrusions. Earth and Planetary Science Letters 219 (3–4), 311–324.

Tao, J.R., 1988. Plant fossils from Liuqu Formation in Lhaze County, Xizang and their palaeoclimatological significances. Monograph of Institute of Geology, Chinese Academy of Sciences, 3. Science Press, Beijing, pp. 223–238 (in Chinese).

Wang, C.S., Li, X.H., Hu, X.M., Jansa, L., 2002. Latest marine horizon north of Qomolangma (Mt. Everest): implications for closure of Tethys seaway and collision tectonics. Terra Nova 1420, 114–120.
Wang, C.S., Liu, Z.F., Li, X.H., Wan, X.Q., 1999. Xigaze Forearc Basin and Yarlung-Zangbo Suture Zone, Tibet. Beijing Geological Publishing House, China. (237 pp.).
Wang, C.S., Liu, Z.F., Hebert, R., 2000. The Yarlung-Zangbo paleo-ophiolite, southern Tibet: implications for the dynamic evolution of the Yarlung-Zangbo Suture Zone. Journal of Asian Earth Sciences 18, 651–661.
Wei, L.J., Liu, X.H., Yan, F.H., Mai, X.S., Zhou, X.J., Li, G.W., Liu, X.B., 2009. Discovery and preliminary study on palynofossils from the Paleogene liuqu conglomerates in southern Xizang (Tibet). Acta Micropalaeontologica Sinica 26 (3), 249–260 (in Chinese with English abstract).
Wen, D.R., Liu, D.Y., Chung, S.L., Chu, M.F., Ji, J.Q., Zhang, Q., Song, B., Lee, T.Y., Yeh, M.W., Lo, C.H., 2008. Zircon SHRIMP U–Pb ages of the Gangdese Batholith and implications for Neotethyan subduction in southern Tibet. Chemical Geology 252 (3–4), 191–201.
Willems, H., Zhou, Z., Zhang, B., Grafe, K.U., 1996. Stratigraphy of the Upper Cretaceous and Lower Tertiary Strata in the Tethyan Himalayas of Tibet (Tingri area, China). Geologische Rundschau 85 (4), 723–754.
Wu, F.Y., Yang, Y.H., Xie, L.W., Yang, J.H., Xu, P., 2006. Hf isotopic compositions of the standard zircons and baddeleyites used in U–Pb geochronology. Chemical Geology 234 (1–2), 105–126.
Wu, F.Y., Clift, P.D., Yang, J.H., 2007. Zircon Hf isotopic constraints on the sources of the Indus Molasse, Ladakh Himalaya, India. Tectonics 26, TC2014. doi:10.1029/2006TC002051.
Wu, F.Y., Ji, W.Q., Liu, C.Z., Chung, S.L., 2010. Detrital zircon U–Pb and Hf isotopic data from the Xigaze fore-arc basin: constraints on Transhimalayan magmatic evolution in southern Tibet. Chemical Geology 271, 13–25.
Xu, Y.G., Lan, J.B., Yang, Q.J., Huang, X.L., Qiu, H.N., 2008. Eocene break-off of the Neo-Tethyan slab as inferred from intraplate-type mafic dykes in the Gaoligong orogenic belt, eastern Tibet. Chemical Geology 255, 439–453.
Yin, A., 2006. Cenozoic tectonic evolution of the Himalayan Orogen as constrained by along-strike variation of structural geometry, exhumation history, and foreland sedimentation. Earth-Science Reviews 76 (1–2), 1–131.
Yin, A., Harrison, T.M., 2000. Geologic evolution of the Himalayan–Tibetan orogen. Annual Review of Earth and Planetary Sciences 28, 211–280.
Yin, A., Harrison, T.M., Murphy, M.A., Grove, M., Nie, S., Ryerson, F.J., Wang, X.F., Chen, Z.L., 1999. Tertiary deformation history of southeastern and southwestern Tibet during the Indo-Asian collision. Geological Society of America Bulletin 111, 1644–1664.
Yin, J.X., Sun, X.X., Sun, Y.X., Liu, C.J., 1988. Stratigraphy on the molasse-type sediments of the paired molasse belts in Xigaze area. Monograph of Institute of Geology, Chinese Academy of Sciences, 3. Science Press, Beijing, pp. 158–176 (in Chinese).
Zhu, B., Kidd, W.S.F., Rowley, D.B., Currie, B.S., Shafique, N., 2005. Age of initiation of the India–Asia collision in the east-central Himalaya. Journal of Geology 113 (3), 265–285.